IEEE Access
Multidisciplinary : Rapid Review : Open Access Journal

Received May 31, 2019, accepted June 21, 2019, date of publication June 26, 2019, date of current version July 18, 2019.

Digital Object Identifier 10.1109/ACCESS.2019.2925139

Rapid Optimization of Battery Charging-Discharging Profiles Using SOC-SOC Rate Domain for Cruising Hybrid Vehicles

JUNYOUNG KIM AND CHANGSUN AHN
School of Mechanical Engineering, Pusan National University, Busan 46241, South Korea

Corresponding author: Changsun Ahn (sunahn@pusan.ac.kr)

This work was supported in part by the National Research Foundation of Korea funded by the Ministry of Science and ICT under Grant NRF-2019R1A2C1003103, and in part by the Industry Core Technology Development Program funded by the Ministry of Trade, Industry and Energy of Korea under Grant 10076309.

ABSTRACT Intelligent use of batteries in hybrid electric vehicles (HEV) is the main factor for high-fuel economy. For a cruising HEV, the state-of-charge Pulse and Glide (SOC-PnG) is known to be the optimal charging–discharging pattern. The optimal charging–discharging profiles of the SOC-PnG strategy can be obtained using the optimization algorithms, such as dynamic programming and Pontryagin's minimum principle. These methods are general tools for optimal control problems but they demand too much computing resources. This paper proposes a problem-specific optimization method that can solve an optimal control problem of the SOC-PnG with less computing resources than the general optimization algorithms. The problem is formulated in the SOC–SOC rate domain, which simplifies the optimization problem and removes many constraints. This approach transforms the necessary conditions for the optimality from one with a path function to one with a point function. An optimization algorithm based on the point function can obtain the optimal solutions about 100 times faster than dynamic programming. This fast optimization is possible because the algorithm exploits the specific cost structure and problem properties. Therefore, this algorithm cannot be applied to all optimization problems but it can accelerate the recursive and time-consuming system design or control design processes in HEV research.

INDEX TERMS Fuel efficiency, hybrid vehicle, optimization, state-of-charge Pulse and Glide (SOC-PnG)

I. INTRODUCTION

As regulations and customers demand higher fuel economy, various related research has been performed. Most general approaches focus on a design aspect, such as weight-reducing technologies. These approaches use new materials or new structures [1]–[3]. Electrification of the powertrain system is also one of the important approaches to increase fuel economy. Hybrid electric vehicles (HEV) achieve a very high level of fuel economy that conventional vehicles cannot reach by adding a battery and motor as additional power sources. The efficiency of an engine is highly dependent on the load and the engine speed. The motor controls the load to the engine or continuously changes the gear ratio so that the engine speed is decoupled from the vehicle speed, which is the basis for the high efficiency of HEV powertrains. Most research on HEVs is on the design of component configurations or optimal power control of a motor and an engine [4]–[9]. Autonomous driving using intelligent transportation system technologies is another potential approach. The vehicle speed of an autonomous vehicle can be a control variable and plays a similar role as the motor of HEVs. A controller can change the velocity or the acceleration of the vehicle so that the engine speed or the engine load is controllable, which can improve the fuel economy.

One of the interesting approaches modulating the vehicle speed for high fuel economy is Pulse and Glide (*PnG*) driving. The approach is based on driving with periodic

The associate editor coordinating the review of this manuscript and approving it for publication was Roberto Sacile.

acceleration followed by deceleration within a speed range, which reduces fuel consumption [10]–[12]. The *PnG* strategy can be applied to HEVs. On a highway, vehicles are in a cruising state for most of the time. For a cruising HEV, charging and discharging of the battery with a *PnG* strategy is known to be optimal and is called the state-of-charge *PnG* (*SOC-PnG*) strategy [13].

Li introduced the Legendre pseudo-spectral method to formulate an optimal control problem to avoid some numerical issues, but the problem was still a mixed integer problem, which requires a significant amount of time to solve the problem. Dynamic Programming (DP) and Pontryagin's Minimum Principle (PMP) are popular methods to solve these types of problems in HEV research [14]–[17]. These methods are general approaches to solve an optimal control problem but require a huge amount of computing resources.

This paper proposes a new numerical method to solve an optimal control problem for *SOC-PnG*. The method is based on a problem defined in a *SOC-SOC rate* domain rather than the *time-SOC* domain, which removes many equality and inequality constraints and transforms the necessary conditions from a path function to a point function. The proposed algorithm finds the optimal solution among a small number of candidate solutions that meet the necessary conditions. The proposed method reduces the computing time required to obtain the optimal solution by approximately 100 times compared to DP.

The rest of the paper is organized as follows. Section II presents the formulation of the optimal control problem for the *SOC-PnG* strategy in the *SOC-SOC rate* domain, and Section III presents how to extract the optimal charging discharging profile for the *SOC-PnG* strategy. Section IV presents some case studies, and Section V concludes the paper.

II. OPTIMAL CONTROL PROBLEM FORMULATION

A. SOC-PnG STRATEGY

The *SOC-PnG* strategy is similar to the *PnG* strategy. The engine of the HEV generates more power during the pulse phase than that used for cruising to operate in an efficient region. The excess power is stored in the battery, so the vehicle does not need to speed up due to the excess power. The engine idles or is turned off during the glide phase but the vehicle still runs at the desired cruising speed because the motor can provide power using the energy stored in the battery during the pulse phase. In the case of HEVs, the vehicle speed does not need to fluctuate, and the SOC fluctuates instead, as shown in Figure 1.

In this chapter, an optimal control problem for the *SOC-PnG* strategy is formulated to achieve the optimal charging-discharging profile for a cruising HEV.

B. VEHICLE MODEL

A mid-sized parallel hybrid electric vehicle is considered, and the variables and parameters are shown in Table 1.

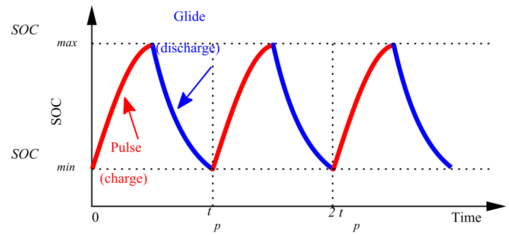

FIGURE 1. SOC trajectory for ***SOC-PnG*** strategy presented in ***time-SOC*** domain.

TABLE 1. Vehicle parameters and variables.

Symbol	Name	Value
N_f	Final gear ratio	3.63
R_w	Wheel radius (m)	0.33
f_{rr}	Rolling resistance coefficient	3.316
f_{aero}	Aerodynamic resistance coefficient	0.52
g	Gravitation acceleration (m/s^2)	9.8
m	Vehicle mass (kg)	1579
N_t	Transmission gear ratio	[2.95, 1.62, 1, 0.68]
C_{batt}	Battery capacitance(Ah)	6
p_g	Transmission gear position	[1, 2, 3, 4]
τ_e	Engine torque (N·m)	
τ_m	Motor torque (N·m)	
ω_e	Engine speed (rpm)	
V_{oc}	Battery open circuit voltage	
V_{batt}	Battery voltage	
I_{batt}	Battery current	
R_{batt}	Battery resistance	
P_{batt}	Battery power	
v	Longitudinal velocity (m/s)	
f	Fuel rate (g/s)	

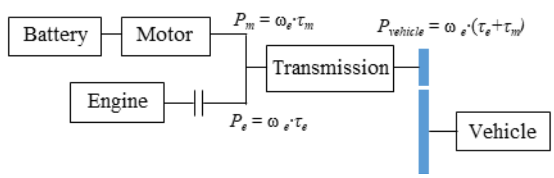

FIGURE 2. Simplified powertrain model of parallel hybrid vehicle.

We consider only longitudinal dynamics with a simplified powertrain shown in Figure 2. The powertrain consists of an engine, motor, battery, transmission, and final gear. Hybrid vehicles have two power sources for driving: one is a battery, and the other is an engine. The power demand for driving is split into two power sources. The overall efficiency is determined by how much and when the power is split. The transmission has four gear positions. When the transmission is in the neutral position, the engine is disconnected from the drivetrain and turned off. For a cruising vehicle, the total force applied to the vehicle is zero, and the vehicle dynamics are:

$$\frac{\tau_e + \tau_m}{R_w} N_f N_t - f_{aero} v^2 - f_{rr} mg = 0. \quad (1)$$

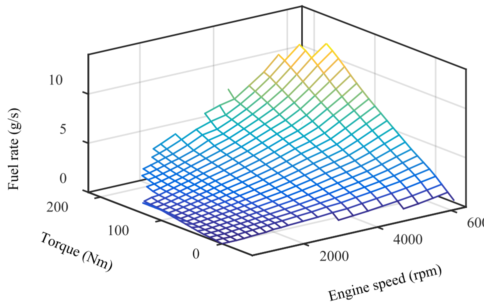

FIGURE 3. Engine fuel rate.

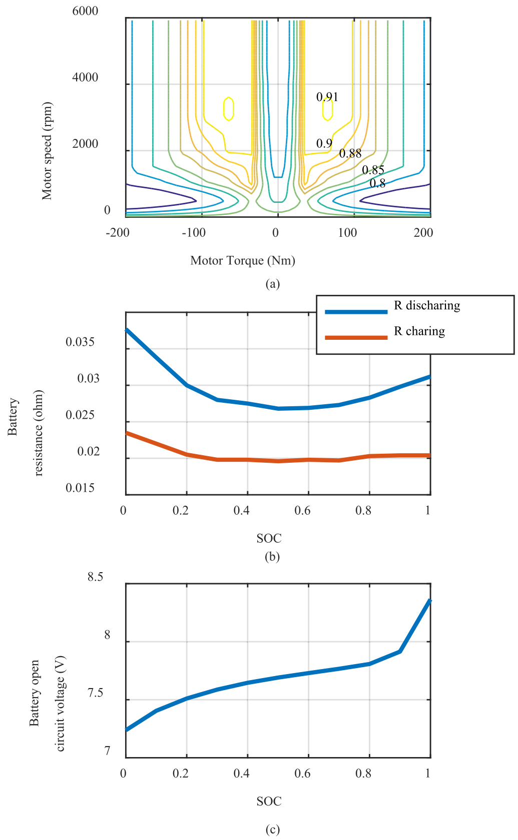

FIGURE 4. Motor and battery characteristics. (a) Motor efficiency, (b) Battery resistance. (c) Battery open circuit voltage.

Given a cruising speed, the total required torque from the engine and the motor is determined using (1).

The engine model is a quasi-static function, as shown in Figure 3. The fuel rate f is expressed as a function of the engine speed ω_e and the engine torque τ_e. The electric components (the motor and battery) are also modeled using quasi-static functions, as shown in Figure 4. The efficiency of the motor is a function of the motor torque and the motor speed that is same as the engine speed unless the engine is disconnected. The open circuit voltage and the internal resistance of the battery are functions of the SOC. The battery dynamics are:

$$S\dot{O}C = -\frac{V_{oc} - \sqrt{V_{oc}^2 - 4\tau_m \omega_e R_{batt}}}{2R_{batt}C_{batt}}. \tag{2}$$

C. FORMULATION OF OPTIMAL CONTROL PROBLEM FOR SOC-PnG IN TIME-SOC DOMAIN

For the *SOC-PnG* driving shown in Figure 1, the cost J for the optimization problem is defined as the fuel consumption in g/m:

$$J = \frac{F_c}{D_c} = \frac{\int_{t_0}^{t_0+t_p} f\,dt}{\int_{t_0}^{t_0+t_p} v\,dt}, \tag{3}$$

where F_c and D_c are the consumed fuel and the travelled distance during a *SOC-PnG* cycle, respectively.

The equality constraints are the longitudinal vehicle dynamics expressed in (1), the SOC dynamics expressed in (2), and the following SOC conditions:

$$\begin{aligned} SOC(t_0) &= SOC(t_p) = SOC_{\min}, \\ \max(SOC(t)) &= SOC_{\max}, \end{aligned} \tag{4}$$

where SOC_{min} and SOC_{max} are the lower and upper bounds of the allowable SOC range.

The inequality constraints are related to the operation limits of the engine, motor, and battery:

$$\begin{aligned} \tau_{e,\min}(\omega_e) &\le \tau_e \le \tau_{e,max}(\omega_e), \\ \tau_{m,\min}(\omega_e) &\le \tau_m \le \tau_{m,max}(\omega_e), \\ \omega_{e,min} &\le \omega_e \le \omega_{e,max}, \\ I_{batt,\min}(SOC) &\le I_{batt} \le I_{batt,\max}(SOC), \\ P_{batt,\min}(SOC) &\le P_{batt} \le P_{batt,\max}(SOC), \\ V_{batt,\min}(SOC) &\le V_{batt} \le V_{batt,\max}(SOC). \end{aligned} \tag{5}$$

The optimal control problem can be summarized as follows:

$$[\tau_m^*(t),\ \tau_e^*(t),\ p_g^*(t),\ t_p^*] = \underset{\tau_m(t),\,\tau_e(t),\,p_g(t),\,t_p}{\arg\min} (J), \quad s.t.\ h(x) = 0,\quad g(x) \le 0, \tag{6}$$

where $h(x)$ is for the equality constraints, and $g(x)$ is for the inequality constraints. This problem is a nonlinear and mixed-integer problem with a free final time, which increases the computing time.

D. FORMULATION OF OPTIMAL CONTROL PROBLEM FOR SOC-PnG IN SOC-SOC RATE DOMAIN

The periodic *SOC-PnG* driving shown in Figure 1 can be re-presented in the *SOC-SOC rate* domain, as shown in Figure 5. Using this domain, the cost function (3) can be re-expressed as follows:

$$\begin{aligned} J &= \frac{F_c}{D_c} = \frac{\oint_{cycle} \frac{f}{S\dot{O}C}\,dSOC}{\oint_{cycle} \frac{v}{S\dot{O}C}\,dSOC}, \\ &= \frac{\int_{Charge} \frac{f}{S\dot{O}C} dSOC + \int_{Discharge} \frac{f}{S\dot{O}C} dSOC}{\int_{Charge} \frac{v}{S\dot{O}C} dSOC + \int_{Discharge} \frac{v}{S\dot{O}C} dSOC}, \\ &= \frac{\int_{soc_{\min}}^{soc_{\max}} \frac{f}{S\dot{O}C} dSOC + \int_{soc_{\max}}^{soc_{\min}} \frac{f}{S\dot{O}C} dSOC}{\int_{soc_{\min}}^{soc_{\max}} \frac{v}{S\dot{O}C} dSOC + \int_{soc_{\max}}^{soc_{\min}} \frac{v}{S\dot{O}C} dSOC}, \end{aligned} \tag{7}$$

where the integral variable is SOC, and the lower and upper limits of the variable are fixed values: SOC_{min} and SOC_{max}.

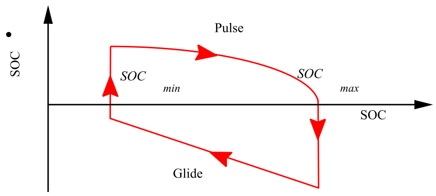

FIGURE 5. SOC trajectory of *SOC-PnG* driving presented in SOC-SOC rate domain.

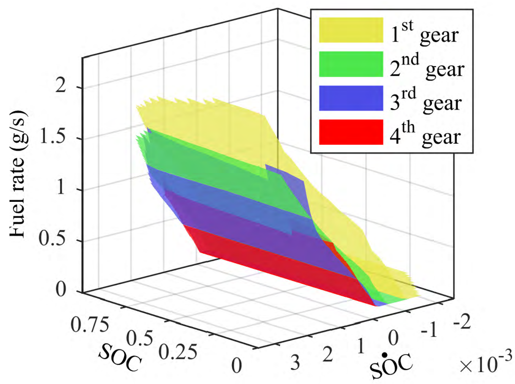

FIGURE 6. Fuel rate in the SOC-SOC rate domain for a cruising vehicle at 60 km/h.

The upper limit of the integral variable in the *Time-SOC* domain (t_p) was not fixed.

Given the SOC rate and SOC, the motor torque and engine torque are determined for a cruising vehicle that is expressed using (1) and (3). Therefore, the fuel rate is determined if the SOC rate, SOC, and gear level are given, as shown in Figure 6. Fuel rate values are results of calculation based on powertrain dynamics and the characteristics of electric components shown in Figures 3 and 4. This figure also shows other interesting features: the optimal gear selection rule. In the *SOC-SOC rate* domain, the optimal gear is easily selected by choosing the gear level with the lowest fuel rate at the given SOC and SOC rate, as shown in Figure 7. Therefore, the gear level is no longer a control variable and is instead dependent on the states. The optimal control problem becomes the following:

$$\begin{aligned} \dot{SOC}^*(SOC) = &\underset{\dot{SOC}(SOC)}{\arg\min}\,(J), \\ &s.t.\ \dot{SOC}_{\min}(SOC) \le \dot{SOC}(SOC) \\ &\quad \le \dot{SOC}_{\max}(SOC). \end{aligned} \tag{8}$$

Through the domain transformation, the control variables are transformed from $[\tau_m,\ \tau_e,\ p_g,\ t_p]$ to the SOC rate. The problem is still a nonlinear problem, but it is no longer a mixed-integer problem or free-final-time problem. In this problem formulation, the inequality constraints become simple. Furthermore, these constraints are already imbedded in Figure 6 and Figure 7, which means the inequality constraints in (9) do not need to be considered explicitly. The equality constraints (1) and (2) are considered when calculating the fuel rate shown in Figure 6. Other equality constraints in (4) are considered as the integral limit in (7). Therefore, many equality and inequality constraints are unnecessary for the formulation in the *SOC-SOC rate* domain.

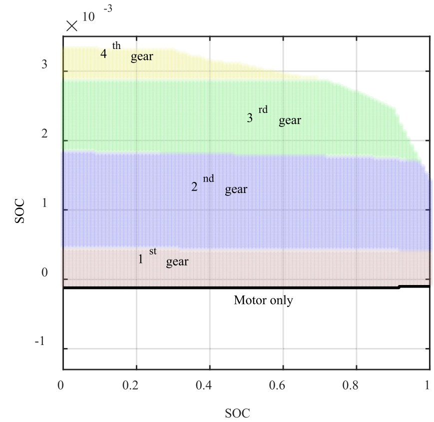

FIGURE 7. Optimal gear selection rule for a cruising vehicle at 60 km/h.

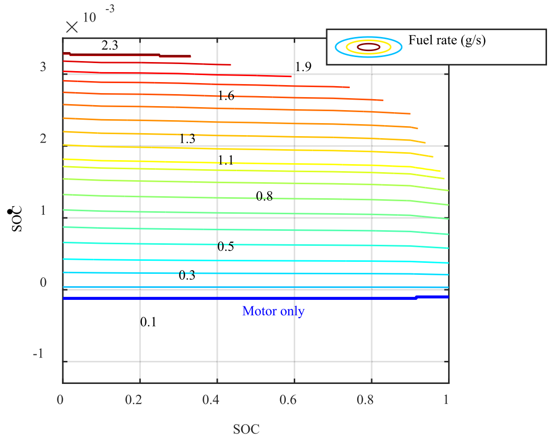

FIGURE 8. Simplified fuel rate function.

The fuel rate function implicitly includes all the constraints. Figure 8 show the fuel rate function when we use optimal gears at each state. Eventually, the optimal control problem becomes:

$$\dot{SOC}^*(SOC) = \underset{\dot{SOC}(SOC)}{\arg\min}\,(J), \tag{9}$$

where

$$J = \frac{\oint_{cycle} \frac{f}{\dot{SOC}}\, dSOC}{\oint_{cycle} \frac{v}{\dot{SOC}}\, dSOC}, \quad f = fuel(SOC, \dot{SOC}).$$

III. EXTRACTION OF OPTIMAL CHARGING DISCHARGING PROFILE

An algorithm is proposed to find an optimal battery charging-discharging profile based on the re-formulated optimal control problem. Figure 9 shows an example of a charging-discharging profile. The closed curve represents a cycle of

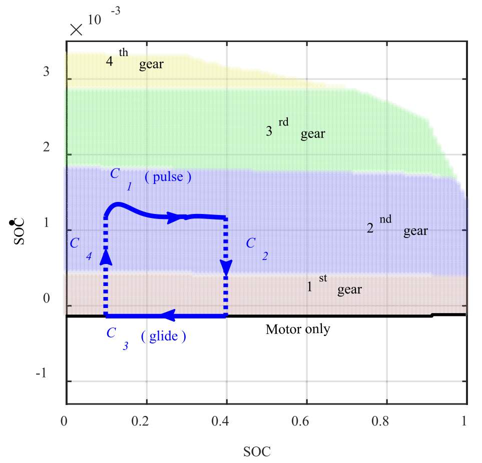

FIGURE 9. ***SOC-PnG* driving cycle in the *SOC-SOC rate* domain.**

SOC-PnG driving. A trajectory C consists of four sections: $C_1 - C_4$. The battery is charged in section C_1 and discharged in section C_3. The lines show the SOC rate as a function of SOC during both the pulse (C_1) and glide (C_3) phases. In sections C_2 and C_4, the SOC rates and SOC changes are zero because the SOC rates change instantaneously from positive to negative, and vice versa. In this cycle, the cost function (10) is expressed as:

$$J = \frac{F_c}{D_c},$$
$$F_c = \int_{C_1} \frac{f}{\dot{SOC}} dSOC + \int_{C_3} \frac{f}{\dot{SOC}} dSOC,$$
$$D_c = \int_{C_1} \frac{v}{\dot{SOC}} dSOC + \int_{C_3} \frac{v}{\dot{SOC}} dSOC. \quad (10)$$

For computational convenience, the problem is transformed into discrete forms as follows:

$$F_c = \sum_{k=1}^{n} \frac{f_k}{\dot{SOC}_k} \Delta SOC + \sum_{k=n+1}^{2n} \frac{f_k}{\dot{SOC}_k} \Delta SOC$$
$$D_c = \sum_{k=1}^{n} \frac{v_k}{\dot{SOC}_k} \Delta SOC + \sum_{k=n+1}^{2n} \frac{v_k}{\dot{SOC}_k} \Delta SOC. \quad (11)$$

The optimal control problem is also transformed as follows:

$$\dot{SOC}^*_{traj} = \underset{\dot{SOC}_{traj}}{\arg\min}(J) = \underset{\dot{SOC}_{traj}}{\arg\min} \left(\frac{F_c(\dot{SOC}_{traj})}{D_c(\dot{SOC}_{traj})} \right), \quad (12)$$

where $\dot{SOC}_{traj} = [\dot{SOC}_1, \cdots, \dot{SOC}_k, \cdots, \dot{SOC}_{2n}]$.

The necessary conditions for the optimality of (12) are:

$$\left. \frac{\partial J}{\partial \dot{SOC}_k} \right|_{\dot{SOC}^*_{traj}} = \left(\frac{\partial F_c}{\partial \dot{SOC}_k} D_c - F_c \frac{\partial D_c}{\partial \dot{SOC}_k} \right) \Big/ D_c^2 \Bigg|_{\dot{SOC}^*_{traj}} = 0 \quad \forall k, \quad (13)$$

or

$$\left. \frac{\partial F_c}{\partial \dot{SOC}_k} \Big/ \frac{\partial D_c}{\partial \dot{SOC}_k} \right|_{\dot{SOC}^*_{traj}} = \left. \frac{F_c}{D_c} \right|_{\dot{SOC}^*_{traj}}, \quad \forall k. \quad (14)$$

The left term in (14) is the ratio between the sensitivity of the consumed fuel to the k^{th} SOC rate and the sensitivity of the travel distance to the k^{th} SOC rate. The right term is the optimal cost or optimal fuel consumption. Using (11), the following equation is derived:

$$\left. \frac{\partial F_c}{\partial \dot{SOC}_k} \Big/ \frac{\partial D_c}{\partial \dot{SOC}_k} \right|_{\dot{SOC}^*_{traj}} = \left(\frac{f_k}{v_k} - \frac{\partial f_k}{\partial \dot{SOC}_k} \frac{\dot{SOC}_k}{v_k} \right) \Bigg|_{\dot{SOC}^*_{traj}}, \quad \forall k. \quad (15)$$

Note that the term on the right hand side is a point function and not a path function. A new function $S(SOC_k, \dot{SOC}_k)$ is defined as a sensitivity ratio function as follows:

$$S(SOC_k, \dot{SOC}_k) = \frac{\partial F_c}{\partial \dot{SOC}_k} \Big/ \frac{\partial D_c}{\partial \dot{SOC}_k} = \frac{f_k}{v_k} - \frac{\partial f_k}{\partial \dot{SOC}_k} \frac{\dot{SOC}_k}{v_k}, \quad (16)$$

and as a result, the necessary condition (14) becomes:

$$S(SOC_1, \dot{SOC}^*_1) = S(SOC_2, \dot{SOC}^*_2) = \ldots \ldots = S(SOC_{2n}, \dot{SOC}^*_{2n}) = \left. \frac{F_c}{D_c} \right|_{\dot{SOC}^*_{traj}}. \quad (17)$$

This is the final form of the necessary condition from which candidates of the optimal charging-discharging profile will be extracted. The last term of (17) happens to be the fuel consumption of the optimal trajectory or the optimal cost. If we know the optimal cost, the optimal trajectory satisfies (17). As mentioned, the function S is a point function, which means that finding a trajectory of SOC that satisfies (17) is not a demanding process. A graphical example is shown in Figure 10.

Figure 10 (a) shows a surface of the sensitivity ratio S as a function of SOC and SOC rate. Assuming an optimal fuel consumption, several trajectories satisfying (17) can be easily extracted, as shown in Figure 10 (b). These trajectories are contour curves that have the same height values (0.01) and are candidates for the optimal trajectory. If the optimal fuel consumption is 0.01, one of the candidates would be the optimal trajectories because they meet the condition, (17). However, the optimal fuel consumption is unknown before the optimal trajectory or the optimal charging-discharging profile is determined, and candidate trajectories should be extracted for all possible values of fuel consumption.

The optimal trajectory must be one of these candidate trajectories extracted using the all possible values. Because the fuel consumption is a physical term, the number of the all possible values is manageably small. By repeating this process for all possible assumed fuel consumption, the optimal trajectory can be achieved.

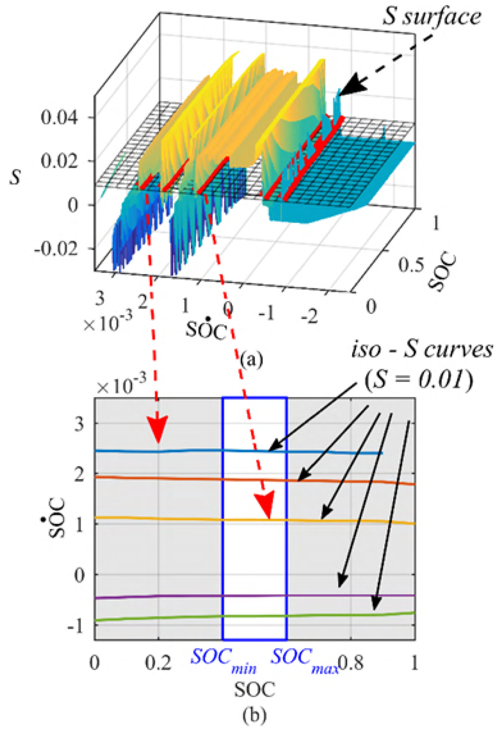

FIGURE 10. **(a) Sensitivity ratio function S, (b) Extraction of contours that have the same S values or the assumed optimal cost (S = J = 0.01).**

IV. ALGORITHM VALIDATION AND DISCUSSION

The proposed algorithm was validated for cases with several cruising speeds. Two cases are shown in Figure 11. To confirm the optimality of the result, DP results are also presented as a reference. Figures 11 (a) and (b) show the charging discharging profiles in the *SOC-SOC rate* domain for speeds of 60 km/h and 120 km/h. Figures 11 (c) and (d) show the profiles on the *time-SOC* domain. Figure 11 (d) presents the fuel consumption. The charging-discharging profiles of both algorithms are almost identical. The fuel consumption shows a slight difference (about 0.2% error) that is from numerical errors because both methods are based on discretization in different domains. Through many comparisons, we confirmed that the proposed algorithm shows almost the same fuel consumption as the DP results.

The computation times for both algorithms are compared in Figure 12. The computation times are presented for cruising cases with several speeds of 30-140 km/h and *SOC-PnG* ranges of 0.45-0.55, 0.4-0.6, and 0.35-0.65 that would be practical ranges for hybrid electric vehicles. Both simulations were performed with the same computer with intel ® Core ™ I7-5500U CPU 2.4 GHz and 8GB RAM. The proposed algorithm required only 1-2 seconds, whereas DP required 150 - 250 seconds. Furthermore, the computing time of DP is quite dependent on the size of the SOC ranges, but the proposed algorithm is less affected by it. These case studies show that the proposed algorithm can achieve the optimal charging-discharging profiles for a cruising HEV under the *SOC-PnG* strategy using less computing time than DP.

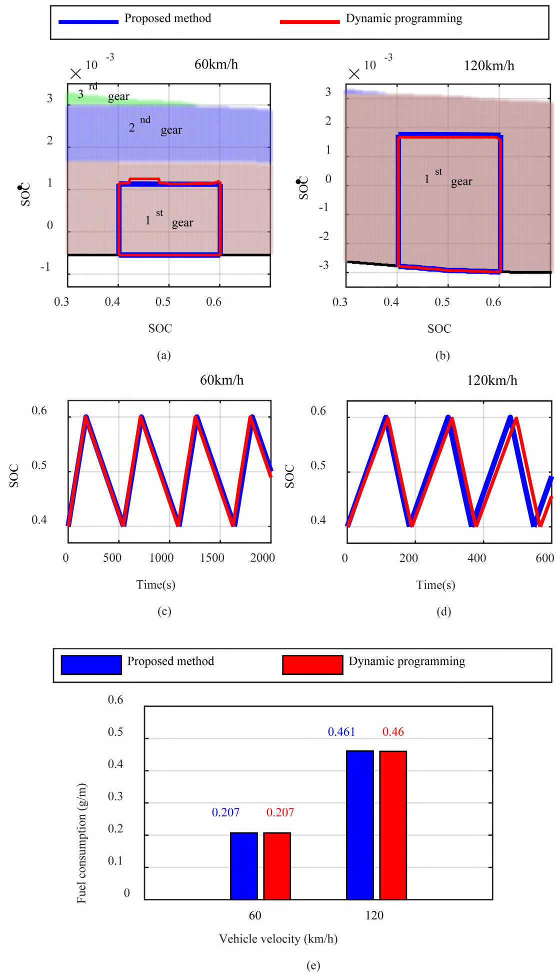

FIGURE 11. **Optimality of the proposed algorithm (a), (b) SOC-PnG trajectories in SOC-SOC rate domain, (c), (d) *SOC-PnG* trajectories in Time-SOC domain, (e) Fuel consumption.**

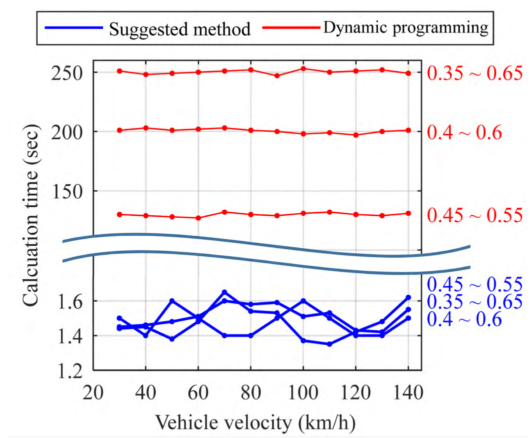

FIGURE 12. **Computation time of the proposed algorithm and DP for various SOC ranges and vehicle velocities.**

The proposed optimization algorithm outperforms DP, but it cannot be applied to all optimization algorithms. The proposed algorithm is problem-dependent and is only valid when one of the system states changes monotonically over time so that the optimization problem can be re-formulated in the new domain with the monotonically changing state. This algorithm was effective for the optimization problem of the *SOC-PnG* strategy because SOC monotonically increases or decreases in that strategy. This algorithm does not have general applicability but shows significant performance improvement in a specific type of optimization problem.

V. CONCLUSION

This paper presented a rapid optimization algorithm to obtain the optimal charging-discharging profiles for a cruising HEV with the *SOC-PnG* strategy. By formulating the optimal control problem for *SOC-PnG* in the *SOC-SOC rate* domain, the problem becomes much simpler than the formulation in the time domain, and many constraints disappear. Using the necessary conditions defined with a point function rather than a path function significantly reduces the complexity. The proposed algorithm reduced the computation time by 100 times compared to DP for the *SOC-PnG* strategy. This approach can be extended to real-time control applications with a small number of control variables or optimization problems with a large number of design variables in cases with monotonic changes of the system states.

REFERENCES

[1] R. Borns and D. Whitacre, "Optimizing designs of aluminum suspension components using an integrated approach," SAE Tech. Paper 2005-01-1387, 2005.

[2] H.-J. Kim, G. A. Keoleian, and S. J. Skerlos, "Economic assessment of greenhouse gas emissions reduction by vehicle lightweighting using aluminum and high-strength steel," *J. Ind. Ecol.*, vol. 15, no. 1, pp. 64–80, Feb. 2011.

[3] A. P. Hardwick and T. Outteridge, "Vehicle lightweighting through the use of molybdenum-bearing advanced high-strength steels (AHSS)," *Int. J. Life Cycle Assessment*, vol. 21, no. 11, pp. 1616–1623, Nov. 2016.

[4] N. Jalil, N. A. Kheir, and M. Salman, "A rule-based energy management strategy for a series hybrid vehicle," in *Proc. IEEE Amer. Control Conf.*, vol. 1, Jun. 1997, pp. 689–693.

[5] G. Paganelli, S. Delprat, T. M. Guerra, J. Rimaux, and J. J. Santin, "Equivalent consumption minimization strategy for parallel hybrid powertrains," in *Proc. IEEE/VTS Spring VTC Conf.*, Birmingham, AL, USA, May 2002, pp. 2076–2081.

[6] J. Liu and H. Peng, "Modeling and control of a power-split hybrid vehicle," *IEEE Trans. Control Syst. Technol.*, vol. 16, no. 6, pp. 1242–1251, Nov. 2008.

[7] J. Lee, D. J. Nelson, and H. Lohse-Busch, "Vehicle inertia impact on fuel consumption of conventional and hybrid electric vehicles using acceleration and coast driving strategy," SAE Tech. Paper 2009-01-1322, 2009.

[8] K. Jeong, S. Ha, and H. Lee, "Supervisory control algorithm design of a 48V 4WD hybrid electric vehicle with fuel efficiency analysis," *Trans. Korean Soc. Automot. Eng.*, vol. 26, no. 1, pp. 131–141, Jan. 2018.

[9] J. Kim and Y.-I. Park, "Fuel economy analysis of novel hybrid powertrain for PHEV," *Trans. Korean Soc. Automot. Eng.*, vol. 27, pp. 325–332, Apr. 2019.

[10] S. E. Li, K. Deng, Y. Zheng, and H. Peng, "Effect of pulse-and-glide strategy on traffic flow for a platoon of mixed automated and manually driven vehicles," *Comput.-Aided Civil Infrastruct. Eng.*, vol. 30, no. 11, pp. 892–905, Nov. 2015.

[11] S. E. Li, X. Hu, K. Li, and C. Ahn, "Mechanism of vehicular periodic operation for optimal fuel economy in free-driving scenarios," *IET Intell. Transp. Syst.*, vol. 9, no. 3, pp. 306–313, Apr. 2015.

[12] S. Xu, S. E. Li, X. Zhang, B. Cheng, and H. Peng, "Fuel-optimal cruising strategy for road vehicles with step-gear mechanical transmission," *IEEE Trans. Intell. Transp. Syst.*, vol. 16, no. 6, pp. 3496–3507, Dec. 2015.

[13] S. Xu, S. E. Li, H. Peng, B. Cheng, X. Zhang, and Z. Pan, "Fuel-saving cruising strategies for parallel HEVs," *IEEE Trans. Veh. Technol.*, vol. 65, no. 6, pp. 4676–4686, Jun. 2016.

[14] C.-C. Lin, H. Peng, J. W. Grizzle, and J.-M. Kang, "Power management strategy for a parallel hybrid electric truck," *IEEE Trans. Control Syst. Technol.*, vol. 11, no. 6, pp. 839–849, Nov. 2003.

[15] N. Kim, S. Cha, and H. Peng, "Optimal control of hybrid electric vehicles based on Pontryagin's minimum principle," *IEEE Trans. Control Syst. Technol.*, vol. 19, no. 5, pp. 1279–1287, Sep. 2011.

[16] J. Jeong, N. Kim, W. Lim, Y.-I. Park, S. W. Cha, and M. E. Jang, "Optimization of power management among an engine, battery and ultra-capacitor for a series HEV: A dynamic programming application," *Int. J. Automot. Technol.*, vol. 18, no. 5, pp. 891–900, Oct. 2017.

[17] N. Kim, J. Jeong, and C. Zheng, "Adaptive energy management strategy for plug-in hybrid electric vehicles with Pontryagin's minimum principle based on daily driving patterns," *Int. J. Precis. Eng. Manuf.-Green Technol.*, vol. 6, no. 3, pp. 539–548, Jul. 2019.